

Representative Time Series Fractal Analysis of the Traffic Flows of a Dedicated High-Speed Link

Ginno Millán Naveas^{1,*}, Román Osorio Comparán²

¹ Universidad de Santiago de Chile,
Departamento de Ingeniería Eléctrica,
Chile

² Universidad Nacional Autónoma de México,
Instituto de Investigación en Matemáticas Aplicadas y en Sistemas,
Departamento de Ingeniería de Sistemas Computacionales y Automatización,
Mexico

ginno.millan@usach.cl, roman@unam.mx

Abstract. The fractal behavior is ubiquitously observed in measurements and characterization of traffic flow in high-speed computer networks of different technologies and coverage levels. This paper presents the results obtained when applying fractal analysis techniques on a time series obtained from traffic captures coming from an application server connected to the Internet through a high-speed link. The results obtained show that traffic flow in the dedicated high-speed network link exhibited fractal behavior since the Hurst exponent was in the range of 0.5, 1, the fractal dimension between 1, 1.5, and the correlation coefficient between -0.5, 0. Based on these results, it is ideal to characterize both the singularities of the fractal traffic and its impulsiveness during a fractal analysis of temporal scales. Finally, based on the results of the time series analysis, the fact that the traffic flows of current computer networks exhibit fractal behavior with a long-range dependency is reaffirmed.

Keywords. Fractals, Hurst exponent (H), long-range dependence (LRD), fractal dimension (D), correlation coefficient (ρ), time series.

1 Introduction

Fractal behavior and LRD are observed in many phenomena, such as in nature [1-6], in financial time series [7], in communication systems traffic [8-12], and in heart rate time series [13,14]. This article characterized the time-series dynamics of traffic flows captured from a high-speed dedicated

link connecting an application server and the Internet, by applying fractal analysis considering the following test: time-scale analysis (TSA), detrended fluctuation analysis (DFA), and power-spectral analysis (PSA).

The data analyzed correspond to the size of traffic frames of the central online applications server at Universidad de Santiago de Chile, which serves 9000 users connected online through the internet. This article analyzes two different types of traffic flows, **SERV-1** and **SERV-2**. **SERV-1** is the temporary series of frame sizes that are transferred to the server from the Internet and **SERV-2** is the temporary series of frame sizes that are transferred from the server to the Internet. These traffic flows play an important role in determining the degree of smooth access to the corresponding application server and therefore the Quality of Service provided to users and the Quality of Experience that users perceive [15,16].

The traffic bursts over extensive periods reveal that the traffic flows under study are identified with a completely different nature from those predicted by a classic Poisson model related to the traffic flows of the old telephone system. For this reason, this research focuses on applying a broad battery of fractal analysis that reaffirms that traffic flow in current high-speed computer networks are fractal with LRD, regardless of their sources such as device requesting services [17]. This research is about a high-speed dedicated link and an on-line

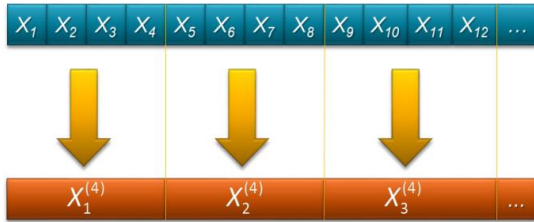


Fig. 1. Aggregation process of non-overlapping segments for a time series

Table 1. Intervals of values for H_E and D and their associated processes

H	D (9)	ρ (7)	FP Behavior
> 0.5	< 1.5	Positive	Persistent
$= 0.5$	$= 1.5$	Random	fBm
< 0.5	> 1.5	Negative	Non-persistent

application server. It should be noted that the time series come from the capture of packets on said link and therefore can be generalized in terms of the presence of traffic from both the Internet and from within the corporate network of the Universidad de Santiago de Chile.

The article is structured as follows. First, we present the general aspects of fractal processes, followed by the key aspects of power-spectral analysis, detrended fluctuation analysis and time-scale analysis. Then the main results obtained are presented and their validity is discussed. Finally, the principal aspects of the research are summarized, and the conclusions are presented.

2 Theoretical Foundation

2.1 Fractal Processes

A Fractal Process (FP) is characterized by having a non-integer dimension, D . In addition, a FP has two characteristics inherent to its phenomenology:

1. A FP is like itself even at different observation scales. This property is known as invariance at the scale. The Self-similarity exists when the process exhibits a similar behavior under an isotropic scaling [18].

2. A FP consists of a complex internal structure and shows the same behavior even in different magnification scales [18], i.e. FP it has a self-similar hierarchical structure.

Due to the scale invariance, a power-law behavior exists in between two parameters in a FP that is governed by the following relationship:

$$f(x) \propto x^c, \tag{1}$$

where $f(x)$ is a function of a study object and c is a constant.

On the other hand in [19] the way of estimating D is exposed based on the power-law behavior expressed by (1). Moreover, from the definition of fractal Brownian motion (fBm) presented in [20] it is necessary that a process fBm is governed by:

$$B_H(t) = [\tau(H+0.5)]^{-1} \left(\int_{-\infty}^0 [(t-s)^{H-0.5} - (-s)] dB(s) + \int_0^t (t-s)^{H-0.5} dB(s) \right), \tag{2}$$

where H is the Hölder exponent of fBm process with $0 < H < 1$.

In addition, $B_H(t)$ satisfies:

$$E[B_H(t)] = 0, \tag{3}$$

$$E[B_H^2(t)] \sim t^{2H}, \tag{4}$$

$$E[B_H(t)B_H(s)] = 0.5(|t|^{2H} + |s|^{2H} - |t-s|^{2H}). \tag{5}$$

From (5) the correlation coefficient, ρ , between $B_H(t)$ increment can be written in the form:

$$\rho = \left\langle \frac{-B_H(-t)B_H(t)}{B_H^2(t)} \right\rangle, \tag{6}$$

where:

- If $t = t_0$, then $B_H(t = t_0) = 0$,
- If $t = -t$, then $B_H(t = -t) = B_H(-t)$,
- $B_H(t) = -B_H(t)$ for all t .

Therefore, we have that:

$$\rho = 2^{2H-1} - 1. \tag{7}$$

Then, be $y(t)$ a FP with Hurst exponent given by H and then for arbitrary process with:

$$y(ct) \triangleq c^H y(t), \quad c > 0, \quad (8)$$

also is a FP with the same statistical distributions that the process $y(t)$, and in which it is verified that D is given by [19]:

$$D = 2 - H. \quad (9)$$

Table 1 shows relationships between H , D , ρ , and the FP behavior.

2.2 Power-Spectral Analysis (PSA)

Time series can be described in the time-domain by $x(t)$, but can also be described in the frequency domain by Fourier Transform (FT), $X(\omega)$, where ω angular frequency. The autocorrelation function of a non-stationary time series $x(t)$, is given by:

$$R_{xx}(t + \tau) = \int_{-\infty}^{\infty} E[x(t)x(t + \tau)]dt, \quad (10)$$

and the FT of this autocorrelation function same with $|X(\omega)|^2$, therefore the power-spectral density (PSD), $S(\omega)$, of a time series can be written as:

$$S(\omega) \triangleq |X(\omega)|^2. \quad (11)$$

Using the Wiener-Khintchine theorem, the PSD of time series can be expressed as the FT of (10) as follows:

$$S_{xx}(\omega) = \int_{-\infty}^{\infty} R_{xx}(\tau) e^{-j\omega\tau} d\tau. \quad (12)$$

The power-spectral function provides an important parameter to characterize the persistence in time series. For a fractal time series, its power-spectral function [19] obey to the frequency based power-law behavior, and given by:

$$S_m(\omega) \sim \omega_m^{-\beta}, \quad \text{with } m = 1, 2, \dots, N/2, \quad (13)$$

where $\omega_m = m/N$, N the length of time series and β is the spectral exponent that characterizes series persistence. The relationship between β , H , and D is given by:

$$\beta = 2H_E + 1 = 5 - 2D. \quad (14)$$

This expression allows us to obtain the value of β using the least-squares method on the adjustment curves of H or D .

The PSA method only provides the value of global H from the FT using a harmonic function. However, it is traditional in fractal analysis for its simplicity to obtain an estimate of the real value of H [21].

2.3 Detrended Fluctuation Analysis (DFA)

The DFA has been widely used to determine the scaling properties of self-similar processes and to determine LRD on noisy and non-stationary time series. In general, this type of analysis is used to estimate the fluctuation of the RMS (Root-Mean-Square) of series with and without trend (this last case is a variant of the analysis of the RMS of the processes based on the theory of random walks [22]), and also because it has the ability to detect LRD. The mathematical form of a time series $Y(i)$, is given according to [23] by:

$$Y(i) = \sum_{k=1}^i (x_k - \langle x \rangle), \quad \text{with } i = 1, \dots, N, \quad (15)$$

where x_k is the sequence k th of the time series of length N , and $\langle x \rangle$ is its average.

Then the series $Y(i)$ given by (15) is regrouped in N_s $\text{Int}(N/s)$ on non-overlapping segments of equal length, s , as shown in Fig. 1, a process also known as aggregation.

As it often happens, the lengths of the time series are not a multiple of the multiple of the time-scale, s , so a short part of it remains at the end of the aggregate series. To solve this problem, the same procedure is repeated but this time starting from the opposite end and analyzing the remaining part at the start of the aggregate series; therefore, the total number of segments is $2N_s$.

After the aggregate time series composed of N_s segments of length s have been obtained, an optimal adjustment line is projected using the last-squares method in each series to obtain the local tendency of each segment that composes it. The deviation of each time series is obtained from the subtraction of line of best fit of minimum squares and the variance is calculated by:

$$F^2(s, v) \equiv \frac{1}{s} \sum_{i=1}^s \{Y[(v-1)s + i] - y_v(i)\}^2, \quad (16)$$

for each segment v , with $v = 1, \dots, N_s$, and:

$$F^2(s, v) \equiv \frac{1}{s} \sum_{i=1}^s \{Y[N - (v - N_s)s + i] - y_v(i)\}^2, \tag{17}$$

for each segment $v = N_s + 1, \dots, 2N_s$, where $y_v(i)$ corresponds to the best adjustment line obtained by using the least-squares method in segment v .

The last step of the DFA analysis is to obtain the average of all segments of each time series disaggregated to find the function given in detail by the equation:

$$F(s) \equiv \frac{1}{2N_s} \sum_{v=1}^{2N_s} F^2(s, v), \tag{18}$$

where $F(s)$ increases as s increases and is defined only for segments of length $s \geq 4$. Therefore, the previous steps are repeated several times to obtain a data set of $F(s)$ versus s , where the slope of the curve obtained from that graph represents the scaling exponent α if the series is correlated according to a long-range power-law.

Therefore, $F(s)$ and s are related by the power-law:

$$F(s) \sim s^\alpha. \tag{19}$$

Table 2 relates the scaling exponent α to different types of processes.

2.4 Time-Scale Analysis (TSA)

The methods presented in the previous sections are based on the development of a linear log-log type graph that only outputs a unique value of the H . These methods are insufficient in estimating the time-dependent Hurst exponent, $H(t)$ [24,25]. The Wavelet Transform approach results in a powerful mathematical tool that serves to real both hierarchy of a FP and spatial distribution of the singularities of the fractal measurements. In this investigation only the Continuous Wavelet Transform (CWT) [26] is considered for temporal scales analysis to estimate $H(t)$ [26]. It should be noted that in the literature H as a global (general) Hurst exponent and $H(t)$ as local Hurst exponent is usual [27,28].

So the CWT is defined as [29]:

$$W_x(t, a, \varphi) = \int_{-\infty}^{\infty} x(s) \varphi_{t,a}^*(s) ds, \tag{20}$$

Table 2. Relationship between α and processes types

α	Process Type
$\in (0, 0.5)$	Power-law anti-correlation
$= 0.5$	White noise
$\in (0.5, 1)$	Long-range power-law correlation
$= 1$	1/f process
> 1	fBm

where φ^* is the conjugate complex of φ function, that for different observations scales is defined as:

$$\varphi_{t,a}(s) = |a|^{0.5} \varphi \left[\frac{s-t}{a} \right], \tag{21}$$

where a is the scale-parameter and $a \propto \omega - 1$.

In this investigation the Morlet Wavelet [30] is used for the TSA and its scalogram is defined as:

$$E_x = \int_{-\infty}^{\infty} \int_{-\infty}^{\infty} |W_x(t, a, \varphi)|^2 a^2 dt da, \tag{22}$$

where E_x is the energy of function x .

Therefore, scalogram is an energy distribution function of a signal in time-scale plane associated with $dt da a^{-2}$. With respect to the above, it should be understood that, in general, any time series is a representation of a signal [31]. Thus considering time series with uniform H can be described as:

$$|x(s) - x(t)| \leq |s - t|^H, \text{ with } c \in \mathbb{R}. \tag{23}$$

Applying CWT for $x(t)$ in (23):

$$|W_x(t, a, \varphi)| \leq |a|^{H+0.5} \int_{-\infty}^{\infty} |t|^H |\varphi(t)| dt, \tag{24}$$

and the scalogram for this time series is given by the following expression [31]:

$$\Omega(t, a) \equiv |W_x(t, a)|^2 \propto |a|^{2H_E(t)+1}, a \rightarrow 0. \tag{25}$$

Based on (25) it is possible to estimate $H(t)$ and write H as follows:

$$H_E = T^{-1} \int_0^T H(t) dt. \tag{1}$$

Thus, the TSA provides both H and $H(t)$.

Table 3. Numerical experiments for **SERV-1** and **SERV-2** time series considering H_E , D , β , and ρ

Temporary Series	H	D	β	ρ
SERV-1	0.70±0.01	1.80±0.01	1.60±0.01	-0.25±0.01
SERV-2	0.71±0.01	1.81±0.01	1.61±0.01	-0.24±0.01

Table 4. Exponent of scaling (α) for different processes

Time Series Type	Hurst Exponent	α according to DFA method	$\pm\alpha$
Brownian Motion	$H = 0.50$	1.20	0.10
Persistence power-law	$H = 0.80$	1.51	0.09
Anti-persistence power-law	$H = 0.20$	1.80	0.03

Table 5. Scaling exponent (α) for **SERV-1** and **SERV-2** time series

Time Series	α_1	$\pm\epsilon$	α_2	$\pm\epsilon$	α_3	$\pm\epsilon$
SERV-1	0.65	0.04	1.08	0.05	2.01	0.05
SERV-2	0.64	0.03	1.07	0.05	2.00	0.04

Table 6. H_E , $\text{Min}\{H_E(t)\}$, $\text{Max}\{H_E(t)\}$, and D for **SERV-1** and **SERV-2**

Time Series	H	$\text{Min}\{H(t)\}$	$\text{Max}\{H(t)\}$	D
SERV-1	0.32	-0.49	1.48	1.68
SERV-2	0.27	-0.26	1.15	1.73

Therefore, the Time-Scale Analysis (TSA) is a more powerful mathematical tool compared to PSA and DFA in FP analysis, since most traffic flows show multifractal scaling behaviors, and it is possible to characterize them with the fluctuations of H described by $H(t)$.

3 Fractal Analysis Development

The power-spectral exponent, H , D , and ρ of the **SERV-1** and **SERV-2** estimated with PSA method are tabulated in Table 3. It is emphasized that the power-spectral exponent is defined in (13) and is related to H and D by means (14); ρ is related to H through (7).

The results clearly show that the **SERV-1** and **SERV-2** time series exhibits fractal behavior with LRD that agrees with the theory.

To test the accuracy of the DFA algorithm which used in this research, the algorithm is used to calculate the scaling exponent of three know scaling exponent generated signals, which are Brownian motion, persistence power-law, and anti-persistence power-law processes with Hurst exponent $H = 0.50$, $H = 0.80$, and $H = 0.20$ [31], respectively. The results are shown in Table 4.

The results show that the scaling exponents obtained are consistent with the H for the three series generated, which verifies that DFA method

carry out the fluctuation analysis without tendency is assertive to reproduce results.

The scaling exponent of **SERV-1** and **SERV-2** series estimated with DFA method are shown in Table 5.

The results show complete coherence with the theory and that the behavior of the time series under study, respond to a fractal character with LRD. The experiment on the scaling exponent reflects both series respond to a behavior of the fractal type with LRD.

The scalogram allows one to estimate the global H and local $H(t)$ Hurst exponents for **SERV-1** and **SERV-2** time series. The results applying the TSA method are summarized in Table 6.

From the results given in Tables 3, 4, 5 and 6, it is shown that the two time series under analysis (**SERV-1** that contains the frame sizes that are transferred to the server from the Internet and **SERV-2** that contains the frame sizes that are transferred from the server to the internet) exhibit fractal characteristics with LRD. It is inferred, therefore, that the increase of samples for any of both series as a result of the extension of the observation time will not result in a modification of their nature, given that these two series have a behavior with LRD.

Even when the Fourier Transform uses harmonic basis functions and the processing of non-stationary signals, the PSA is a good way to start with the initial measurements of non-stationary time series that are suspected to have a fractal nature, as is the case of the time series presented in this investigation.

Two of the main results obtained are:

- $H = 0.70 \pm 0.01$ in **SERV-1** time series,
- $H = 0.67 \pm 0.01$ in **SERV-2** time series.

Results that show that both series respond to a fractal character with LRD.

It is interesting to examine the results of the analysis of fluctuation without tendency, since they show that both time series present the characteristic crossing phenomenon described in [11].

In relation to the origin of this phenomenon, it can be explained from the fact that there are very short times between a service request and the server's response. This generates time series for a

highly fluctuating uncorrelated process. As the time passes the signals show fluctuations that tend to soften, reflecting the dynamics of every current telecommunications system, resulting in an exponent $\alpha = 1$ associated with a process $1/f$.

The results of TSA show that the considered time series are constitutive of extremely complicated systems that present a time-dependent Hurst exponent which ranges from negative to positive values $-0.50 \leq H(t) \leq 1.50$ for the **SERV-1** series and $-0.30 \leq H(t) \leq 1.15$ for the **SERV-2** series. It is further noted that $H(t)$ for the **SERV-1** series has greater complexity than $H(t)$ for the **SERV-2** series. This difference can find an explanation in the following. For **SERV-1**, the data comes from thousands of points distributed on the internet to a server entry port, which will create a bottleneck in the server gateway. In addition, there is interaction between incoming signals and outgoing signals on the gateway during the period when the input signal is overloaded and causes network congestion. On the other hand, the **SERV-1** series turns out to be more regular since the data is transferred from the main gateway to thousands of points distributed on the internet, this transfer is clearly simpler compared to the case of incoming traffic.

Since $H(t)$ for series under study are outside the range $-0.50 \leq H(t) \leq 1.50$, they are very complicated systems that merit independent study to obtain a better description, both quantitative and qualitative.

Notwithstanding the above, the TSA provides valuable information in comparison with the PSA and the DFA fact that allows us to study in detail the behavior of the complex system considered consisting of recorded data traffic flows from and to the internet from an online application server.

4 Conclusions

A detailed analytical study on long-range fractality and dependence for two time series of traffic has been presented. The series labeled **SERV-1** and **SERV-2** are examined by three methods: PSA, DFA and TSA.

It is made clear that there are other techniques to examine LRD that are not addressed in this

investigation, such as dispersion analysis and maximum likelihood estimators.

The main results are summarized as follows:

1. The PSA reports that the series are fractal and have LRD given that the following conditions:

β : $1 < \beta < 2$, H : $0.5 < H < 1$; ρ : $-0.5 < \rho < 0$, and D : $1 < D < 2$.

2. The analysis of fluctuation without trend shows that the series present the characteristic cross phenomenon of fractal processes with long-range dependence [11].

3. The TSA reports that the time series under study, **SERV-1** and **SERV-2**, present a time-dependent Hurst exponent, outside the range (0, 1). Therefore, these time series require an advanced quantitative as well as qualitative description to improve the understanding of the series of internet traffic coming from a high demand environment as it is an online application server, it is more, it is recorded that $H(t)$: $-0.5 \leq H(t) \leq 1.5$, H : $0.5 < H < 1.0$, and D : $1 < D < 2$.

Finally, it is demonstrated that fractality and LRD are presented in the series under study that represent traffic captures from a high-speed dedicated link.

Acknowledgments

This work was developed thanks to the support of the Instituto de Investigaciones en Matemáticas Aplicadas (IIMAS) of the Universidad Nacional Autónoma de México (UNAM) through the use of the equipment for the Laboratorio Universitario de Cómputo de Alto Rendimiento (LUCAR).

The authors would especially like to thank their administrator, Esp. Adrián Durán Chavesti, for his cooperation and support.

References

1. **von Korff, M., Sander, T. (2019)**. Molecular Complexity Calculated by Fractal Dimension. *Cientific Reports*, Vol. 9. DOI: 10.1038/s41598-018-37253-8.
2. **Berstein, S., Hoffmann, M. (2019)**. Climate Politics, Metaphors and the Fractal Carbon Trap. *Natural Climate Change*, Vol. 9, pp. 919–925. DOI: 10.1038/s41558-019-0618-2.
3. **Igbawua, T., Zhang, J., Yao, F., Ali, S. (2019)**. Long Range Correlation in Vegetation over West Africa from 1982 to 2011. *IEEE Access*, Vol. 7, pp. 119151–119165. DOI: 10.1109/ACCESS.2019.2933235.
4. **Nie, Q., Shi, K., Gong, Y., Ran, F., Li, Z., Chen, R., Hua, L. (2020)**. Spatial-temporal Variability of Land Surface Temperature Spatial Pattern: Multifractal Detrended Fluctuation Analysis. *IEEE Journal of Selected Topics in Applied Earth Observations and Remote Sensing*, Vol. 13, pp. 2010–2018. DOI: 10.1109/JSTARS.2020.2990479.
5. **Pan, H., Zhang, W., Jiang, W., Wang, P., Yang, J., Zhang, X. (2020)**. Roughness Change Analysis of Sea Surface from Visible Images by Fractals. *IEEE Access*, Vol. 8, pp. 78519–78529. DOI: 10.1109/ACCESS.2020.2990161.
6. **Cipolletti, M.P., Genchi, S.A., Delrieux, C., Perillo, G.M.E. (2020)**. An Approach for Estimating Border Length in Marine Coasts from MODIS Data. *IEEE Geoscience and Remote Sensing Letters*, Vol. 17, No. 1, pp. 8–12. DOI: 10.1109/LGRS.2019.2916620.
7. **Karaca, Y., Zhang, Y.D., Muhammad, K. (2020)**. Characterizing Complexity and Self-similarity Based on Fractal and Entropy Analyses for Stock Market Forecast Modeling. *Expert Systems with Applications*, Vol. 144. DOI: 10.1016/j.eswa.2019.113098.
8. **Millán, G., Kaschel, H., Lefranc, G. (2010)**. Discussion of the Analysis of Self-similar Teletraffic with Long-range Dependence (LRD) at the Network Layer Level. *International Journal of Computers, Communications & Control*, Vol. 5, No. 5, pp. 799–812. DOI: 10.15837/ijccc.2010.5.2240.
9. **Millán, G., Lefranc, G. (2015)**. Application of the Analysis of Self-similar Teletraffic with Long-range Dependence (LRD) at the Network Layer Level. *Int. Journal of Computers, Communications & Control*, Vol. 10, No.1, pp. 62–69.
10. **Fontugne, R., Abry, P., Fukuda, K., Veitch, D., Cho, K., Borgnat, P., Wendt, H. (2017)**.

- Scaling in Internet Traffic: a 14 Year and 3 Day Longitudinal Study, with Multiscale Analyses and Random Projections. *IEEE/ACM Trans. Networking*, Vol. 25, No. 4, pp. 2152–2165. DOI: 10.1109/TNET.2017.2675450.
11. **Millán, G., San Juan, E., Vargas, M. (2019).** A Simplified Multifractal Model for Self-similar Traffic Flows in High-speed Computer Networks. *Computación y Sistemas*, Vol. 23, No. 4, pp. 1517–1521. DOI: 10.13053/cys-23-4-2831.
 12. **Tian, Z. (2020).** Chaotic Characteristic Analysis of Network Traffic Time Series at Different Time Scales. *Chaos, Solitons & Fractals*, Vol. 130. DOI: 10.1016/j.chaos.2019.109412.
 13. **Korolj, A., Wu, H.-T., Radisic, M. (2019).** A Healthy Dose of Chaos: Using Fractal Frameworks for Engineering Higher-fidelity Biomedical Systems. *Biomaterials*, Vol. 219. DOI: 10.1016/j.biomaterials.2019.119363.
 14. **Zhang, D., Wang, C., Li, C., Dai, W. (2019).** Multi-Fractal Detrended Fluctuation Half-spectrum Analysis of HRV. *The Journal of Engineering*, Vol. 2019, No. 22, pp. 8315–8318. DOI: 10.1049/joe.2019.1067.
 15. **Li, J., Lin, J. (2019).** Research on the Influence of Sampling Methods for the Accuracy of Web Services QoS Prediction. *IEEE Access*, Vol. 7, pp. 39990–39999. DOI: 10.1109/ACCESS.2019.2906769.
 16. **Bouraqla, K., Sabir, E., Sadik, M., Ladid, L. (2020).** Quality of Experience for Streaming Services: Measurements, Challenges and Insights. *IEEE Access*, Vol. 8, pp. 13341–13361. DOI: 10.48550/arXiv.1912.11318.
 17. **Millán, G., Lefranc, G. (2009).** Presentation of an Estimator for the Hurst Parameter for a Self-similar Process Representing the Traffic in IEEE 802.3 networks. *International Journal of Computers & Control*, Vol. 4, No. 2, pp. 137–147. DOI: 10.15837/ijccc.2009.2.2421.
 18. **Millán, G., Fuertes, G., Alfaro, M., Carrasco, R., Vargas, M. (2018).** *IEEE International Conference on Automation / XXII Congress of the Chilean Association of Automatic Control*, pp. 1–4.
 19. **Fernández-Martínez, M., Rodríguez-Bermúdez, G., Vera, J.A. (2017).** On Discrete Models of Fractal Dimension to Explore the Complexity of Discrete Dynamical Systems. *Journal of Difference Equations and Applications*, Vol. 23, No.1–2, pp. 258–274. DOI: 10.1080/10236198.2016.1216550.
 20. **Granero-Belichón, C., Roux, S.G., Garnier, N.B. (2019).** Information Theory for Non-stationary Processes with Stationary Increments. *Entropy*, Vol. 21, No. 12, pp. 1223. DOI: 10.3390/e21121223.
 21. **Lan, H., White, P.R., Li, J., Sn, D. (2020).** Coherent Averaged Power Spectral Estimate for Signal Detection. *Signal Processing*, Vol. 169. DOI: 10.1016/j.sigpro.2019.107414.
 22. **Xia, F., Liu, J., Nie, H., Fu, Y., Wan, L., Kong, X. (2020).** Random Walks: A Review of Algorithms and Applications. *IEEE Transactions on Emerging Topics in Computational Intelligence*, Vol. 4, No. 2, pp. 95–107. DOI: 10.1109/TETCI.2019.2952908.
 23. **Zhang, X., Liu, H., Zao, Y., Zhang, X. (2019).** Multifractal Detrended Fluctuation Analysis on Air Traffic Flow Time Series: a single Airport Case. *Physica A: Statistical Mechanics and its Applications*, Vol. 531. DOI: 10.1016/j.physa.2019.121790.
 24. **Bianchi, S., Pianese, A. (2018).** Time-varying Hurst-Hölder Exponents and the Dynamics of (in)Efficiency in Stock Markets. *Chaos, Solitons & Fractals*, Vol. 109, pp. 64–75. DOI: 10.1016/j.chaos.2018.02.015.
 25. **Mollaei, S., Darooneh, A.H., Karimi, S. (2019).** Multi-scale Entropy Analysis and Hurst Exponent. *Physica A: Statistical Mechanics and its Applications*, Vol. 528. DOI: 10.1016/j.physa.2019.121292.
 26. **Garcin, M. (2017).** Estimation of Time-dependent Hurst Exponents with Variational Smoothing and Application to Forecasting Foreign Exchange Rates. *Physica A: Statistical Mechanics and its Applications*, Vol. 483, pp. 462–479. DOI: 10.1016/j.physa.2017.04.122.
 27. **Molino-Minero-Re, E., García-Nocetti, F., Benitez-Pérez, H. (2015).** Application of a Time-Scale Local Hurst Exponent Analysis to

- Time Series. *Digital Signal Processing*, Vol. 37, pp. 92–99. DOI: 10.1016/j.dsp.2014.11.007.
- 28. Lotfalinezhad, H., Maleki, A. (2020).** TTA, a New Approach to Estimate Hurst Exponent with Less Estimation Error and Computational Time. *Physica A: Statistical Mechanics and its Applications*, Vol. 553. DOI: 10.1016/j.physa.2019.124093.
- 29. Keerthana, Y.M., Reddy, M.K., Rao, K.S. (2019).** CWT-Based Approach for Epoch Extraction from Telephone Quality Speech. *IEEE Signal Processing Letters*, Vol. 26, No. 8, pp. 1107–1111. DOI: 10.1007/s10772-022-10013-w.
- 30. Cohen, M.X. (2019).** A Better Way to Define and Describe Morlet Wavelets for Time-frequency Analysis. *NeuroImage*, Vol. 199, pp. 81–86. DOI: 10.1016/j.neuroimage.2019.05.048.
- 31. Boashash, B. (2016).** *Time Frequency Signal Analysis and Processing. A Comprehensive Reference.* Academic Press: UK.

Article received on 27/08/2020; accepted on 16/02/2025.

**Corresponding author is Ginno Millán Naveas.*